Journal of http://www.satursonpublishing.com/
Research in Multidisciplinary Methods and Applications
ISSN 2957-3920 (Online) ISSN 3007-7060 (Print)
Volume 4, Issue 4, April 2025

Study on Corrosion Resistance of SERMETEL Coating

Jingwen Qiu

North China University of Water Resources and Electric Power. Zhengzhou, China

* Corresponding to. Jingwen Qiu

Abstract: Using 17-4PH steel with good toughness and castability, easy to press and weld as the base material, SERMETEL water based high temperature resistant coating for coating, the 17-4PH stainless steel surface after surface cleaning is coated with a part of the shot peening method of first coating the bottom coating and then coating the sealing coating, the other part is coated with primer coating to dry after sand blasting treatment and then coated with sealing coating. The service performance of the coating was tested by continuous spray resistance to synthetic seawater, heat/synthetic seawater salt spray cycle test and electrochemical test, after 100h SERMETEL coating shot blasting and sandblasting treatment, obvious corrosion occurred on the surface of the sample, and the color of the sample surface became dark, and scattered pitting pits were visible. The pitting pits on the surface of the samples of synthetic seawater continuously sprayed for 1000h were enlarged and connected into sheets. Serious corrosion has occurred on the surface of the 1000h synthetic seawater continuous spray sample, after the combined alternating action of high temperature and seawater salt spray, the surface of the sample has a relatively obvious and large corrosion trace, especially the specimen edges corrosion is more serious, the coating corrosion exposed the substrate, and the substrate appeared obvious rust color. The self-corrosion potential and self-corrosion current density of SERMETEL coated 17-4PH stainless steel samples treated with shot blasting and sandblasting were determined by electrochemical experiments in different concentrations of NaCl solution. Found shot peening and sandblasting coating corrosion rate is the fastest in 5% NaCl solution.

Keywords: stainless steel; coating; harsh environment; wear resistance and corrosion resistance.

1 INTRODUCTION

Phosphate, as an inorganic material, has good high temperature resistance, however, its application technology is more complex, mainly used in aerospace and other special fields and casting fields [1,2]. Initially, the phosphate binder is cured without curing agent, and the curing temperature is usually 400-500℃,with the continuous progress of related research, phosphate binders began to be cured with curing agents in the 1990s,the curing temperature of the binder system decreases from 400-500℃ to 190℃,now the application of inorganic high temperature resistant phosphate coatings and related composite materials in China is less.[3,4,5,6,7]At present, high temperature resistant composite material prepared by high temperature resistant phosphate binder is widely used in radar radome, in the late 1950s, due to the good electromagnetic wave transmission and thermal shock resistance of phosphate-based materials, they could meet the performance requirements of high-speed aircraft radomes, and relevant research and results began to emerge one after another.[8]In the 1960s, researchers began to study and promote low-cost high-temperature resistant phosphate-based composites, especially for high-performance phosphate curing and careful brushing, the inorganic high temperature resistant phosphate-related materials can be cured at temperatures below 300 °C, and can maintain good comprehensive mechanical properties at ambient temperatures up to 650 °C.[9]Inorganic phosphate is used as an inorganic coating because its phosphorus exists in the form of phosphate ions in the solution, and has many significant advantages over other coatings in terms of performance, and is widely used in various industries. Because it has good heat resistance, corrosion resistance, oil resistance, high temperature resistance and other characteristics. It has a good effect on the protection of the machine, and its coating can be applied to mechanical metal equipment as anti-corrosion materials under high humidity, wear-resistant materials, and refractory materials under high temperature [10,11,12]. At present, the coating using inorganic phosphate as a coating has been widely used in aerospace development, Marine ship manufacturing, automotive new energy industry and other fields and has achieved ideal results. The world's commercial inorganic high temperature resistant aluminum-phosphate anti-corrosion coatings can provide good surface protection when the coating thickness is 50μm,the research found that according to the salt spray atmosphere corrosion test standard of the American Society for Material Testing, the

Journal of http://www.satursonpublishing.com/
Research in Multidisciplinary Methods and Applications
ISSN 2957-3920 (Online) ISSN 3007-7060 (Print)
Volume 4, Issue 4, April 2025

water-based aluminum phosphate coating can withstand more than 3000h salt spray corrosion test, has excellent corrosion protection and high temperature oxidation resistance, and can be used for the surface protection of the blade in the low temperature section of the engine, it can also replace the cadmium-plated titanium technology for surface protection of aircraft landing gear parts and fasteners[13,14,15]. However, because the related coatings can be applied to sensitive areas, the relevant technical information of this type of coatings is relatively small.

Continuous spray resistance test to synthetic seawater, heat/synthetic seawater salt spray cycle test and electrochemical experiment for SERMETEL water-based high temperature resistant coating can make up for the relevant research on corrosion and wear resistance of SERMETEL water-based high temperature resistant coating. For such a widely used phosphate coating, it can contribute to its preparation and application in industry. It is of great significance to provide some guidance and reference [16].

2 COATING ANTICORROSION MECHANISM

The anticorrosion mechanism of coatings mainly includes three categories: shielding of corrosive medium, chemical passivation and electrochemical protection. Corrosive medium shielding refers to the surface protection method that the coating on the surface of the metal substrate can prevent the corrosive medium in the surrounding environment from spreading to the metal substrate, so as to avoid the corrosion of metal materials. Chemical passivation refers to the passivation of strong oxidizing additives or fillers in the coating on the surface of the metal material, and the passivation of the surface of the metal matrix, so as to avoid metal corrosion. Electrochemical protection is mainly the use of low-potential metal materials as fillers for corrosion protection of metal materials, the low-potential metal is corroded as an anode in the corrosion process, and the protected workpiece is used as the galvanic battery cathode, which is protected by sacrificing the low-potential metal anode for corrosion protection.

The main anticorrosive mechanism of the water-based aluminum-containing phosphate anticorrosive coating studied in this paper is corrosion medium shielding and chemical passivation, when chromium-containing primer paint is sprayed onto the surface of the substrate and forms a porous aluminum phosphate coating, the porous coating can prevent the coating from peeling off the substrate surface due to the difference in thermal expansion coefficient between the coating and the metal substrate. Meanwhile, the chromium passivator in the primer paint will passivate the surface of the metal substrate, forming a passivation film. After the topcoat paint is cured, it will form a continuous and dense aluminum coating on the surface of the primer paint. The topcoat coating effectively seals the pores of the primer coating and forms a dense aluminum phosphate protective coating with the primer coating on the surface of the high-strength steel.

3 EXPERIMENT

3.1 EXPERIMENTAL MATERIALS

The material used in the experiment is 17-4PHB steel.17-4PHB steel is a commonly used low carbon steel, the yield strength is generally between 235-245MPa, with high strength and corrosion resistance, better welding performance and processing performance, widely used in construction, machinery manufacturing, highways and Bridges and other fields, its chemical composition includes carbon, silicon, manganese, sulfur, phosphorus, etc., the specific composition is shown in the following table：

TABLE 1 EXPERIMENTAL MATERIAL COMPOSITION (%)

C	Si	Mn	S	P	Other
≤0.22	≤0.35	≤1.40	≤0.045	≤0.045	Fe

SERMETEL coating is made by brushing a high temperature resistant top paint composed of silicone, high temperature resistant fillers, auxiliaries and organic solvents [17,18]. Main characteristics It has good heat resistance and can withstand the high temperature of 200℃ for a long time; it has good adhesion; the paint film is resistant to moisture and oil; it has good weather resistance; it can be directly constructed on substrate at high temperature of 200° C. For boiler, engine shell, exhaust pipe, chimney, oven and other high temperature equipment, pipeline temperature less than 200℃ steel surface use [19].

The construction method is divided into two steps: spraying and brushing. Highly pressure airless spray. The use of gas spraying should pay attention to adjust the viscosity of the coating and air pressure. The diluent should not exceed 10%, otherwise the coating performance will be affected. It is used in pre-coating and small area coating, but the specified dry film thickness must be reached. The method used in this test is to distribute sand blasting and shot blasting on the bottom layer after the spray base material is dry, and then apply top paint on the surface of the bottom layer after sand blasting and shot blasting.

3.2 SAMPLE PRETREATMENT

Pre-cleaning of test pieces Dip the test piece into petroleum ether, gently wipe the test piece with the absorbent cotton or medical gauze held with tweezers, wipe clean and dry with hot air;

Test piece grinding in the dry condition, the uncoated surface of the test piece is polished step by step with 150-1000 grit paper, and the grinding direction is parallel along the short edge, that is, the parallel direction of the two holes;

Cleaning of test pieces the polished test piece is repeatedly washed with clean water to remove surface impurities and sand particles, and then ultrasonic cleaning in anhydrous ethanol and acetone alternately for 5 minutes, 3 times each, until the grinding

Journal of http://www.satursonpublishing.com/
Research in Multidisciplinary Methods and Applications
ISSN 2957-3920 (Online) ISSN 3007-7060 (Print)
Volume 4, Issue 4, April 2025

chips, sand particles and other pollutants on the test piece are washed away. For the test pieces coated with inorganic coating, it is not necessary to polish them, but to rinse them with clean water repeatedly, and then ultrasonic cleaning them in anhydrous ethanol and acetone alternately for 5 minutes 3 times each;

Drying of the test piece the cleaned test piece is dried with hot air and cooled to room temperature;

Preservation of test pieces If the test cannot be done immediately, the test piece should be stored in the dryer. However, samples stored for more than 24 hours should be re-polished.

4 Experimental Content

4.1 Resistance To Synthetic Seawater Continuous Spray Test

The synthetic seawater spray was kept at 35±2℃ for 100h and 1000h, respectively. After the test is completed, see if there is breakage or severe corrosion spread in the area where the coating is cut. After the test was completed, the coating (crossed sample: cut place) was observed to see if there was damage or serious corrosion, and the structure, thickness, composition and corrosion products of the coating were observed and analyzed by scanning electron microscopy, energy spectrum and X-ray diffraction to obtain the influence of the above exposure environment on the coating.

4.2 Heat Resistant/Synthetic Seawater Salt Spray Cycle Test

A cycle of "heating 2h at 450℃ in air circulation oven, air cooling to room temperature, and then exposure to synthetic seawater salt spray at 35±2℃ for 20h" was carried out for 10 consecutive cycles. After the test was completed, the surface damage and corrosion spread of the paint film were observed, and the structure, thickness, composition and microstructure of the coating test plate and corrosion products were tested and analyzed by scanning electron microscopy and energy spectrum, so as to obtain the influence of the above exposure environment on the coating.

4.3 Electrochemical Test

On the electrochemical workstation, 23±2℃ synthetic seawater and 3.5%wt sodium chloride solution (the concentration of sodium chloride solution can be adjusted appropriately) were used as electrolytes to test the polarization curve and the open circuit potential was used as the measuring potential, and the AC impedance test was carried out in the frequency range of 0.01 to 100 kHz. The electrochemical characteristics and impedance response of the coating were analyzed by electrochemical tests on the electrochemical workstation.

5 Result Analysis

5.1 Analysis Of Physical And Chemical Properties Of SERMETEL Coating

Fig. 1a Shows The Surface Morphology Of The Sample Treated With SERMETEL Coating. As Can Be Seen From The Figure, The Surface Of The Inorganic Phosphate Coating Is Relatively Flat And The Whole Is Wavy. In Addition, The Surface Of The Coating Was Relatively Flat At High Magnification, And No Cellular Protrusions Were Observed.

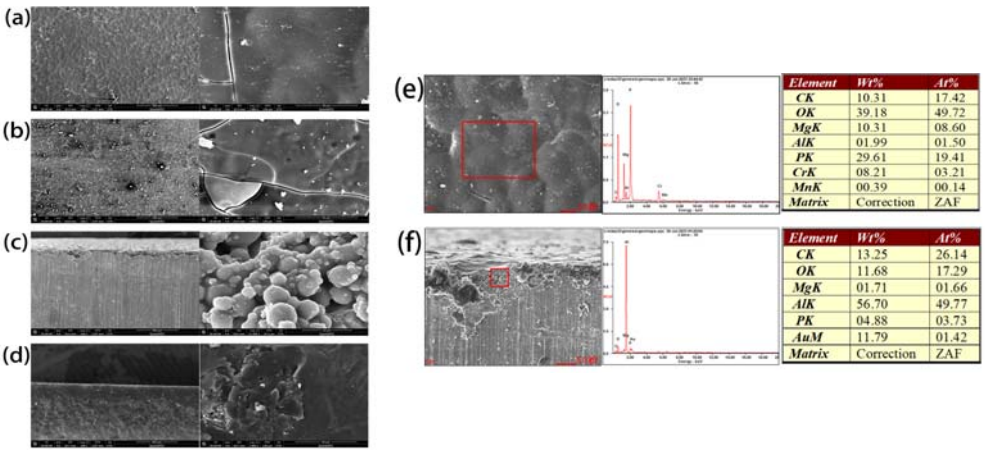

Element	Wt%	At%
CK	10.31	17.42
OK	39.18	49.72
MgK	10.31	08.60
AlK	01.99	01.50
PK	29.61	19.41
CrK	08.21	03.21
MnK	00.39	00.14
Matrix	Correction	ZAF

Element	Wt%	At%
CK	13.25	26.14
OK	11.68	17.29
MgK	01.71	01.66
AlK	56.70	49.77
PK	04.88	03.73
AuM	11.79	01.42
Matrix	Correction	ZAF

Figure.1 (a) SEM Morphology Of 17-4PH Stainless Steel Specimen Coated With SERMETEL Coating Shot Peening. (b) SEM Surface Morphology Of 17-4PH Stainless Steel Sample Coated With SERMETEL Coating And Sandblasted. (c) Cross-Section Morphology Of The Sample Treated With SERMETEL Coating. (d) Cross Section Morphology Of Sandblasted Samples Coated With SERMETEL Coating. (e)(f) The Surface And Cross-Sectional EDX Spectra Of The Shot-Peened Sample Coated With SERMETEL Coating Respectively

Journal of http://www.satursonpublishing.com/
Research in Multidisciplinary Methods and Applications
ISSN 2957-3920 (Online) ISSN 3007-7060 (Print)
Volume 4, Issue 4, April 2025

Fig. 1b shows the surface morphology of sandblasted samples coated with SERMETEL coating. As can be seen from the figure, the surface of the inorganic phosphate coating is relatively flat on the whole, and more fine cracks can be seen in the entire field of view. Considering that this is caused by the drying shrinkage of the coating and the temperature change during the preparation of the coating, signs of cracks can be seen locally. In addition, the surface of the coating was relatively flat at high magnification, and no cellular protrusions were observed.

Fig. 1c shows the cross-section morphology of the sample treated with SERMETEL coating. As can be seen in the figure, the coating is relatively thin, and the binding of the substrate can be seen a clear line. The inside of the coating is relatively loose, in the form of stacking particles, with more internal pores.

Fig. 1d Cross section morphology of sandblasted samples coated with SERMETEL coating. In the figure, it can be seen that the coating and the substrate are tightly bonded, and the inside of the coating is relatively dense, but cracks and local fragmentation of the coating can be seen, which should be hot cracks that appear under the influence of temperature during the preparation of the coating.

Fig 1e and 1f show the surface and cross-sectional EDX spectra of the shot-peened sample coated with SERMETEL coating respectively. The spectrum shows that the main chemical elements in the coating are O, C, Cr, P, Mg, and Al. From the metal element content, the Mg element content is greater than the Cr element content, which is greater than the Al element content, suggesting that the original composition is a composite coating of aluminum chromate and magnesium dihydrogen phosphate. At a certain temperature, the coating decomposes into a composite coating of P2O5, Al2O3, Cr2O3, and MgO.

5.2 Continuous Spray Test Of Synthetic Seawater Resistance

The synthetic seawater spray was kept at 35±2℃ for 100h and 1000h, respectively. After the test is completed, see if there is breakage or severe corrosion spread in the area where the coating is cut. After the test is completed, the coating (crossed sample: where it is cut) is observed for damage or severe corrosion to obtain the effect of the above exposure environment on the coating.

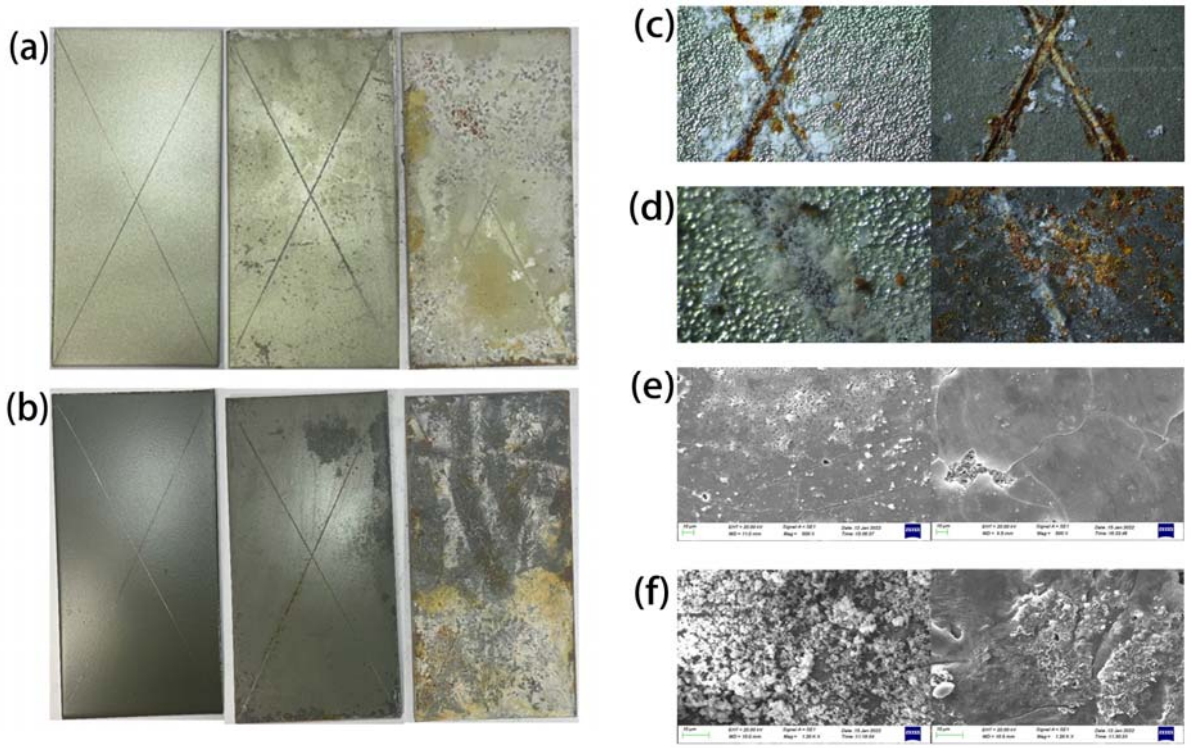

Figure 2. (a)(b) Macroscopic photograph of the surface of 17-4PH stainless steel specimen coated with SERMETEL coating shot peening and sandblasting treatment after synthetic seawater spray test. (c)(d) Metallographic photographs of the surfaces of 17-4PH stainless steel samples coated with SERMETEL coating and sandblasted before and after being kept 100h and 1000h at 35±2℃ synthetic seawater spray respectively. (e)(f) SEM images of surfaces of 17-4PH stainless steel samples coated with SERMETEL coated shot peening and sandblasting after 100 hours and 1000 hours of synthetic seawater spray tests.

Figure 2a b shows the macroscopic photos of the surfaces of 17-4PH stainless steel samples coated with SERMETEL coating and sandblasted before and after the synthetic seawater spray at 35±2°C and kept for 100h and 1000h respectively. As can be seen from the figure, relatively serious corrosion has occurred on the surface of the sample of synthetic seawater continuous

Journal of http://www.satursonpublishing.com/
Research in Multidisciplinary Methods and Applications
ISSN 2957-3920 (Online) ISSN 3007-7060 (Print)
Volume 4, Issue 4, April 2025

spraying for 1000h, and the surface of the sample is covered by thick sedimentary salt layer.

Figure 2 c d shows metallographic photographs of the surfaces of 17-4PH stainless steel samples coated with SERMETEL coating and sandblasted before and after being kept 100h and 1000h at 35±2℃ synthetic seawater spray respectively. As can be seen from the figure, after 100h continuous salt spray test of synthetic seawater, no obvious traces of rust were seen on the surface of the sample, and there was some adhesion of deposited salt particles at the crossing, and traces of matrix corrosion, showing brown corrosion products.

Figure 2e f SEM images of surfaces of 17-4PH stainless steel samples coated with SERMETEL coated shot peening and sandblasting after 100 hours and 1000 hours of synthetic seawater spray tests. Whether it's 100 hours of spray, or 1,000 hours of continuous spray. The surface of the shot peening samples is coated with a layer of seawater dissolved salt, and there is a coating crack propagation and fragmentation. On the other hand, the surface of sandblasted samples showed serious corrosion, and the coating fell off.

5.3 *Heat Resistant/Synthetic Seawater Salt Spray Cycle Test*

Heat resistant/synthetic seawater salt spray cycle is a cycle of "air circulation oven heating for 2h at 450 ° C, air cooling to room temperature, and then exposed to synthetic seawater salt spray at a temperature of 35±2 ° C for 20h for 10 consecutive cycles. After the test was completed, the surface damage and corrosion spread of the paint film were observed, and the influence of the above exposure environment on the coating was obtained.

Figure 3a b displays the macroscopic images of the surface of 17-4PH stainless steel samples prior to and following SERMETEL coating. These samples underwent a heat/synthetic seawater salt spray cycle test, along with shot blasting and sandblasting treatment. It can be seen that after the combined alternating action of high temperature and seawater salt spray, relatively obvious corrosion traces appear on the surface of the sample, especially the corrosion of the sample edge is relatively serious, and the coating corrosion exposes the substrate, and the substrate appears obvious rust color. In contrast, SERMETEL coated sandblasting sample corrosion is more serious than SERMETEL coated shot blasting sample.

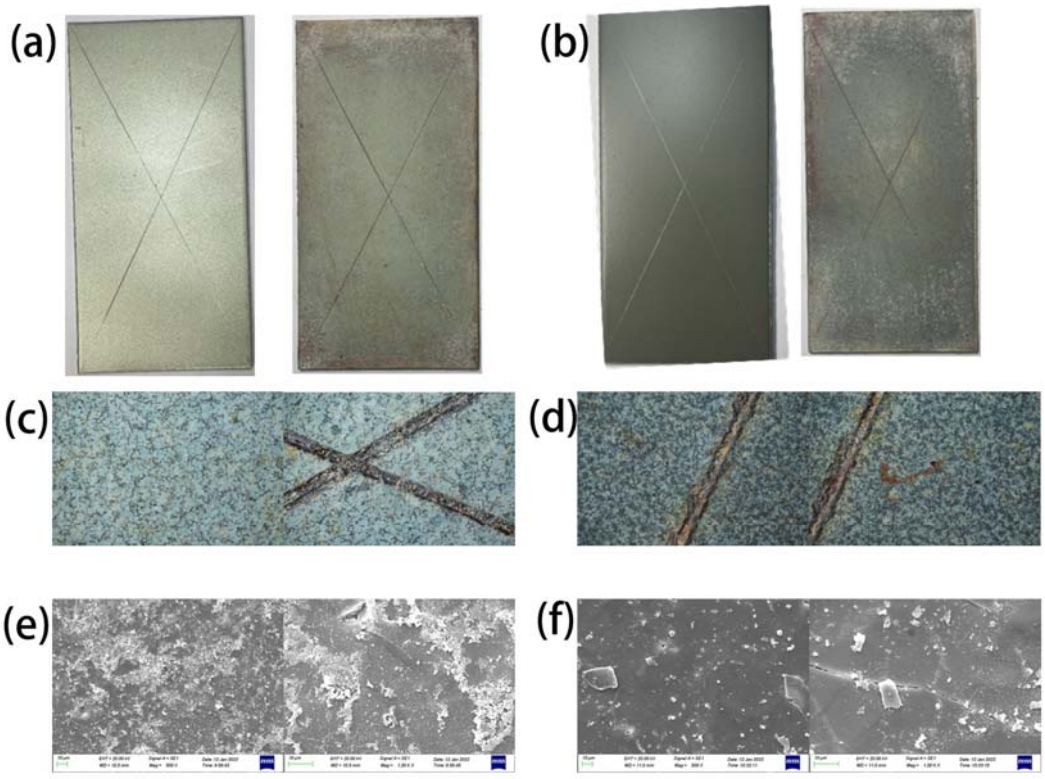

Figure 3. (a)(b) The macro-photos of shot peening and sand blasting were taken before and after the experiment (c)(d) The metallographic photos of shot peening and sand blasting were taken before and after the experiment (e)(f) The scanning electron microscope (SEM) images of shot peening and sand blasting after heat resistance and salt spray test were obtained

Fig. 3c d is a metallographic photograph of the surface of 17-4PH stainless steel specimen coated with SERMETEL coating shot blasting and sandblasting before and after heat resistant/synthetic seawater salt spray cycle test. In the figure, there is no obvious coating peeling phenomenon on the surface, and more corrosion products accumulate at the crossing.

Journal of http://www.satursonpublishing.com/
Research in Multidisciplinary Methods and Applications
ISSN 2957-3920 (Online) ISSN 3007-7060 (Print)
Volume 4, Issue 4, April 2025

Fig. 3e is a SEM photo of the surface of 17-4PH stainless steel specimen coated with SERMETEL coating after a heat resistant/synthetic seawater salt spray cycle test. After 10 cycles of heat resistant/synthetic seawater salt spray cycle, more salt in seawater is dissolved and deposited on the surface of the sample.

Fig. 3f is a SEM photo of the surface of 17-4PH stainless steel sample coated with SERMETEL coating sandblasted after heat resistant/synthetic seawater salt spray cycle test. After 10 cycles of heat resistance/synthetic seawater salt spray cycle, the surface cracks deepened and fell off.

5.4 ELECTROCHEMICAL TEST

5.4.1 SAMPLE PREPARATION

The sample size is 10×10×10mm as shown in Figure 5, The working area of the electrochemical test is 1cm2. The stranded copper wire is pasted on the back of the sample with conductive copper tape. The non-working surface is encapsulated with epoxy resin except for the working surface.

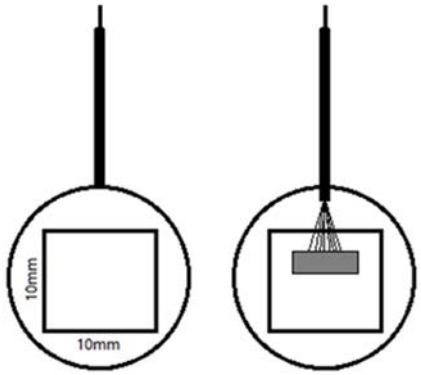

FIGURE 4. SCHEMATIC DIAGRAM OF ELECTROCHEMICAL SAMPLE PREPARATION

5.4.2 ELECTROCHEMICAL TEST

The electrochemical test was carried out on the 760e electrochemical workstation of Chenhua, using a three-electrode system, 17-4PH stainless steel sample coated with SERMETEL coating shot blasting and sandblasting and the test piece uncoated with rust remover as the working electrode, platinum sheet as the auxiliary electrode, saturated calomel electrode (SCE) as the reference electrode. The test solutions are 1%, 3.5%, 5% NaCl solution by mass fraction and synthetic seawater solution. When preparing NaCl solution, deionized water and analytically pure grade NaCl reagent in line with national standards are used; Sodium chloride, magnesium chloride, magnesium sulfate, calcium chloride, potassium chloride, sodium bicarbonate and sodium bromide were added to the deionized water. The contents of each salt were as follows: sodium chloride: 26.50 g/L; Magnesium chloride: 2.40g /L; Magnesium sulfate: 3.30g /L; Calcium chloride: 1.10 g/L; Potassium chloride: 0.73 g/L; Sodium bicarbonate: 0.20g /L; Sodium bromide: 0.28 g/L.Analytical pure reagent was used for each component. The items of open circuit potential, polarization curve and AC impedance were selected respectively for electrochemical test.

（1）Open circuit potential test

The open circuit potential is also called the potential time curve, which refers to the curve of the open circuit potential change over time between the working electrode and the reference electrode, and can be used to detect the natural corrosion potential [20]. Natural corrosion potential is an important thermodynamic parameter for corroding metal electrodes, which is of great significance in studying metal corrosion behavior and analyzing corrosion process, and is widely used in anti-corrosion engineering technology [21,22]. For example, combining potential-pH diagram to judge the corrosion tendency of metal; Judging the polarity of metal in galvanic corrosion; The characteristic potential and sensitive potential interval of some local corrosion were determined. In cathodic protection engineering, as an important technical parameter and criterion.

After the sample was soaked in the solution for 30min and reached the stable state, the open circuit potential was tested. The test time was 300s, and the fluctuation of the open circuit potential was less than 5mV. The open circuit potential of each sample in the stable section was recorded.

（2）Electrochemical impedance test

Electrochemical AC impedance spectroscopy is to measure the change of impedance with the sine wave frequency, and then analyze the electrode process dynamics, double electric layer and diffusion, etc., to study the electrode materials, solid electrolytes, conductive polymers and corrosion protection mechanisms [23,24,25]. Electrochemical impedance spectroscopy is to apply a small amplitude AC potential wave with different frequencies to the electrochemical system, and measure the ratio of AC potential and current signal with the change of sine wave frequency ω, or the phase Angle of the impedance Φ with the change of ω. The electrochemical system is regarded as an equivalent circuit, which is composed of basic components such as resistance (R), capacitor (C) and inductor (L) in different ways such as series parallel combination. Through EIS, the composition of the equivalent circuit and the size of each component can be determined, and the electrochemical meaning of these components can be used to analyze the structure of the electrochemical system and the properties of the electrode process [26].

The frequency range of the electrochemical impedance spectroscopy test was 10mHz-100kHz, the AC excitation signal was a sine wave with a amplitude of 10mV, and the measured potential was an open circuit potential. The fitting analysis of the electrochemical impedance spectroscopy data was carried out by using ZSimpWin software, and the fitting circuit model was established to further calculate the charge transfer resistance.

（3）Polarization curve test

The polarization curve represents the relationship between electrode potential and polarization current or polarization

Journal of http://www.satursonpublishing.com/
Research in Multidisciplinary Methods and Applications
ISSN 2957-3920 (Online) ISSN 3007-7060 (Print)
Volume 4, Issue 4, April 2025

current density. If the electrodes are anode or cathode, the resulting curves are called anode polarization curves respectively (anodic polarization curve) Or cathode polarization curve (cathodic polarization curve) [27,28]. The polarization curve is divided into four regions: active dissolution region, transition passivation region, stable passivation region and over passivation region. The polarization curve can be measured by experimental method. The analysis of polarization curve is one of the basic methods to explain the basic law of metal corrosion, reveal the mechanism of metal corrosion and discuss the way to control corrosion. The polarization curve with the electrode potential as the horizontal coordinate and the current passing through the electrode as the vertical coordinate is called the polarization curve. It characterizes the functional relationship between the driving force potential of the corrosion galvanic cell reaction and the reaction velocity current. The experimental polarization curve is measured directly from the experiment. The relationship between potential and current of individual electrode reaction on local anode or local cathode is called the true polarization curve, that is, the ideal polarization curve.

The scanning rate was 0.5mV /s, the scanning range was ± 0.5mV, the Tafel curve was obtained, and the self-corrosion potential and self-corrosion current density were recorded. The corrosion rate was calculated by the extrapolation method of Tafel curve [29]. The corrosion rate is calculated as follows:

$$\frac{A \times I_{corr}}{n \times F \times \rho} \times 87600 \quad (1)$$

Where A is the atomic weight; Icorr is the self-corrosion current density, expressed in units of A/cm2; n is the number of electrons transferred in the electrochemical reaction; and F is Faraday's constant (1F = 28.6 A·h). ρ is the density of the metal, expressed in units of g/cm3.

5.4.3 Comparison Of Electrochemical Tests In Different Concentrations Of NaCl Solutions

Fig. 5 ab shows the open circuit potential of SERMETEL coated shot peening and sandblasting treated samples in 1%, 3.5% and 5% NaCl solutions, respectively. SERMETEL coatings with shot peening and sandblasting have the highest open circuit potential in 1% NaCl solution and the lowest open circuit potential in 5% NaCl solution. This indicates that with the increase of NaCl solution concentration, the corrosion effect on SERMETEL coatings treated with shot peening and sandblasting is gradually enhanced.

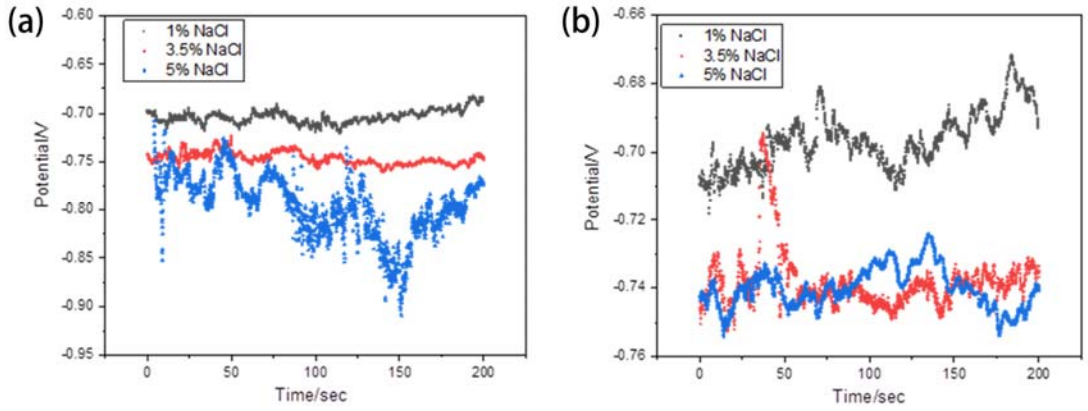

Figure 5. (a) Comparison Of Open Circuit Potentials Of 17-4PH Stainless Steel Samples Coated With SERMETEL Coating And Shot Peening In NaCl Solutions Of Different Concentrations. (b) Comparison Of Open Circuit Potentials Of 17-4PH Stainless Steel Samples Coated With SERMETEL Coating And Sandblasted In NaCl Solutions Of Different Concentrations

Fig. 6a and b show the polarization curves of the samples coated with SERMETEL coating in shot blasting and sandblasting solutions with different concentrations of NaCl. It can be seen from the figure that the coatings treated by SERMETEL shot blasting and sandblasting in different concentrations of NaCl solutions have obvious passivation characteristics. Table 2 shows the self-corrosion potential and self-corrosion current density obtained by fitting the polarization curve. The level of self-corrosion potential represents the difficulty of corrosion of the sample. The higher the self-corrosion potential is, the less electrochemical corrosion will occur, and the lower the self-corrosion potential is, the more electrochemical corrosion will occur. The higher the self-corrosion current density, the faster the corrosion rate of the sample. With the increase of NaCl solution concentration, the self-corrosion potential value of the coating treated with SERMETEL shot peening did not decrease, indicating that the coating treated with SERMETEL shot peening was not sensitive to NaCl concentration, and the corrosion tendency did not increase. The self-corrosion potential value of the coating treated with SERMETEL sandblasting showed an overall decreasing trend, indicating that the corrosion tendency increased with the increase of NaCl concentration. In addition, in different concentrations of NaCl solutions. The self-corrosion potential of SERMETEL shot peening coating is higher than that of SERMETEL sandblasting coating. This shows that the SERMETEL shot peening coating is less prone to corrosion than the SERMETEL sandblasting coating. The self-corrosion current density of the coating treated with

Journal of http://www.satursonpublishing.com/
Research in Multidisciplinary Methods and Applications
ISSN 2957-3920 (Online) ISSN 3007-7060 (Print)
Volume 4, Issue 4, April 2025

SERMETEL shot peening is the highest when the concentration of NaCl solution is 1%. However, the self-corrosion current density decreased with the increase of NaCl concentration, The reason is that obvious electrochemical corrosion occurs when NaCl concentration is 1%. And when NaCl concentration increases, the passivation of the coating prevents further corrosion. The self-etching current density of the coating treated with SERMETEL shot peening generally increased with the increase of NaCl solution concentration, this indicates that the increase of ions in the solution accelerates the corrosion, Passivation did not play an effective protective role.

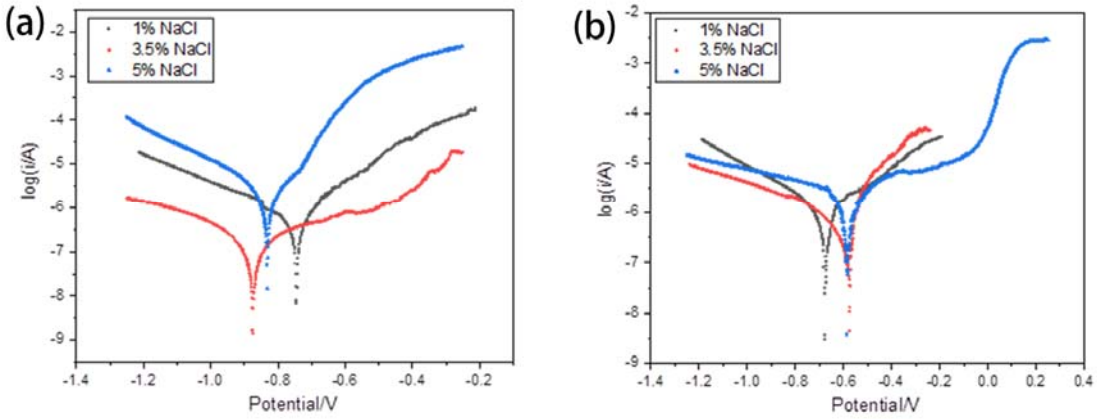

FIGURE 6. (A) COMPARISON OF POLARIZATION CURVES OF 17-4PH STAINLESS STEEL SAMPLES COATED WITH SERMETEL COATING SHOT PEENING IN NACL SOLUTIONS OF DIFFERENT CONCENTRATIONS. (B)COMPARISON OF POLARIZATION CURVES OF 17-4PH STAINLESS STEEL SAMPLES COATED WITH SERMETEL COATING AND SANDBLASTED IN NACL SOLUTIONS OF DIFFERENT CONCENTRATIONS.

TABLE 2 POLARIZATION CURVE FITTING DATA

	Sample number	Self-corrosion potential Corr (V)	Self-etching current density Corr (A/cm2)
1% NaCl Solution	Sha	-0.675	1.523×10-6
	Wan	-0.744	6.624×10-7
3.5% NaCl Solution	Sha	-0.575	2.816×10-7
	Wan	-0.874	1.641×10-7
5% NaCl Solution	Sha	-0.587	3.103×10-6
	Wan	-0.832	1.651×10-6

Table 2 shows the self-corrosion potential and self-corrosion current density obtained by fitting the polarization curve. The level of self-corrosion potential represents the difficulty of corrosion of the sample, The higher the self-corrosion potential is, it is not easy to have electrochemical corrosion, The lower it is, the easier it is to have electrochemical corrosion. The 17-4PH stainless steel sample coated with SERMETEL has the lowest self-corrosion potential. This indicates that 17-4PH stainless steel samples coated with SERMETEL coating are more prone to electrochemical corrosion. The self-corrosion current density is used to characterize the speed of corrosion process, that is, the corrosion rate, from the perspective of kinetics. Fig. 7abcd shows the Bode diagram and Nyquist diagram of AC impedance of 17-4PH stainless steel samples coated with SERMETEL coating in shot blasting and sandblasting solutions at different concentrations of NaCl, respectively. Due to the poor conductivity of the inorganic phosphate coating, the impedance map data points are relatively scattered in the low frequency stage. The AC impedance is fitted, and the fitting circuits are all R(CR) type (see Figure 8). The fitted data are listed in Table 3. Charge transfer resistance (Rct) reflects the charge transfer resistance between the electrode surface and the reactant in solution. The value of charge transfer resistance is related to the reaction rate of the electrode surface, so it can be used to evaluate the reaction performance of the electrode surface.

As shown in Table 3, with the increase of NaCl concentration, the charge-reaction resistance values of the samples coated with SERMETEL coating after shot peening and sandblasting decreased as a whole, indicating that the resistance of charge transfer and transfer on the coating surface decreased with the increase of NaCl concentration, and the corrosion of the coating increased accordingly.

Journal of http://www.satursonpublishing.com/
Research in Multidisciplinary Methods and Applications
ISSN 2957-3920 (Online) ISSN 3007-7060 (Print)
Volume 4, Issue 4, April 2025

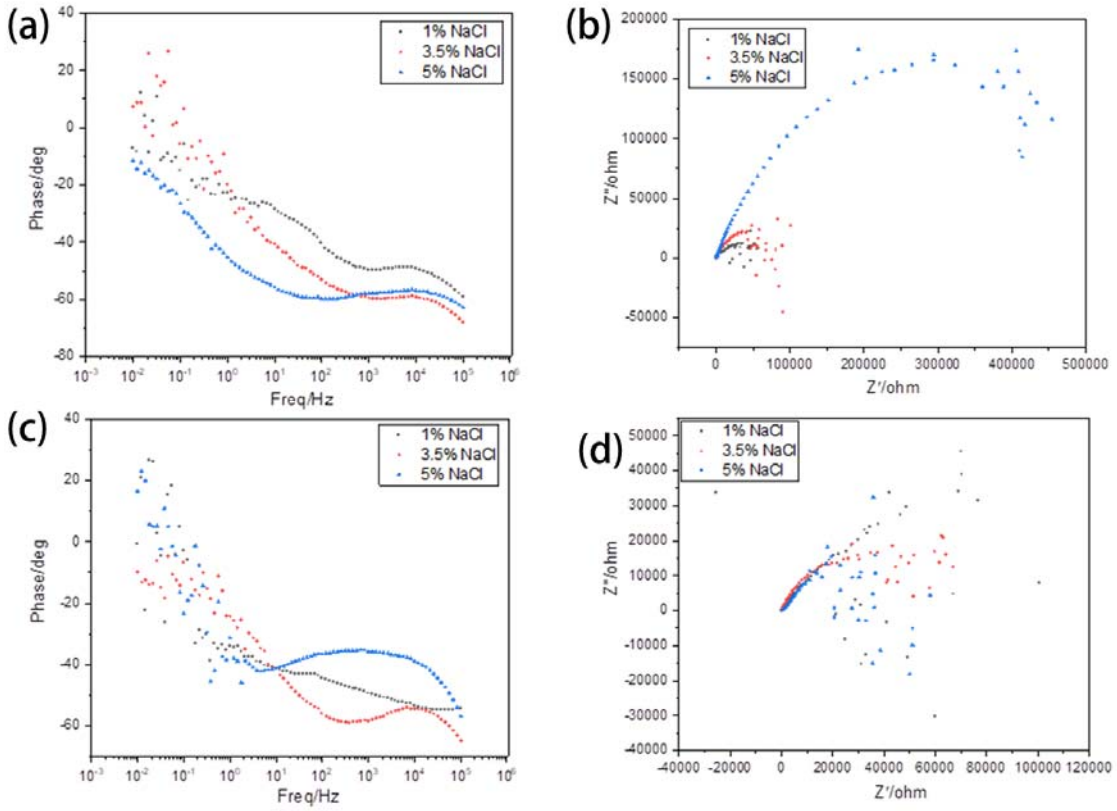

FIGURE 7. (A) AC IMPEDANCE SPECTRA OF 17-4PH STAINLESS STEEL SAMPLES COATED WITH SERMETEL COATING IN DIFFERENT CONCENTRATIONS OF NACL SOLUTION (BODE DIAGRAM). (B) AC IMPEDANCE SPECTRA OF 17-4PH STAINLESS STEEL SAMPLES COATED WITH SERMETEL COATING IN DIFFERENT CONCENTRATIONS OF NACL SOLUTION (NYQUIST DIAGRAM). (C) AC IMPEDANCE SPECTRA OF 17-4PH STAINLESS STEEL SAMPLES COATED WITH SERMETEL COATING IN DIFFERENT CONCENTRATIONS OF NACL SOLUTION (BODE DIAGRAM). (D) AC IMPEDANCE SPECTRA OF 17-4PH STAINLESS STEEL SAMPLES COATED WITH SERMETEL COATING IN DIFFERENT CONCENTRATIONS OF NACL SOLUTION (NYQUIST DIAGRAM).

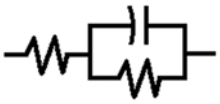

FIGURE 8. AC IMPEDANCE FITTING CIRCUIT

TABLE 3 AC IMPEDANCE FITTING DATA

	Sample number	Rs	C	Rct
1% NaCl Solution	Sha	498.2	18.62×10-	0.596×105
	Wan	430.1	11.48×10-	0.3613×105
3.5% NaCl Solution	Sha	233.3	18.00×10-	0.65×105
	Wan	216.6	9.30×10-8	0.74×105
5% NaCl Solution	Sha	1396	1.609×10-6	3.612×104
	Wan	620.3	1.326×10-7	3.868×105

REFERENCES

[1] Mu, Z., Tang, RK., Liu, ZM. Construction of Inorganic Bulks through Coalescence of Particle Precursors. Nanomaterials, 2022, 11(1).

[2] Xie, LN., Li, YH., Hu, WJ., Fang, SQ., Chen, XQ. A novel inorganic phosphate-based adhesive for bonding archaeological pottery: a preliminary exploration. Heritage science, 2024, 12(1).

[3] Chiou, Jeng-Maw. Improving the temperature resistance of aluminum-matrix composites by using an acid phosphate binder. State University of New York at Buffalo, 2023.

[4] Jia, YL., Wan, HQ., Chen, L., Zhou, HD., Chen, JM. Effects of phosphate binder on the lubricity and wear resistance of graphite coating at elevated temperatures. Surface & coatings technology, 2017, 315, 490-497.

[5] Wang, MC., Dong, X., Zhou, QJ., Feng, ZJ., Liao, YL., Zhou, XM., Du, MR., Gu, YQ. An engineering ceramic-used high-temperature-resistant inorganic phosphate-based adhesive self-reinforced by in-situ growth of mullite whiskers. Journal of the european ceramic society, 2019, 39(4), 1703-1706.

[6] Wang, MC., Liu, JC., Du,HY., Guo, AR., Tao,X., Dong, X., Geng, HT. A SiC whisker reinforced high-temperature resistant phosphate adhesive for bonding carbon/carbon composites. Journal of Alloys and Compounds, 2015, 633, 145-152.

[7] Darba,GB., Aliofkhazraei,M. Electrochemical phosphate conversion coatings: a review. Materials transactions, 2017, 24(03), 1730003.

[8] El Aggadi, S., Ennouhi, M., Boutakiout, A., El Hourch, A. Progress towards efficient phosphate-based materials for sodium-ion batteries in electrochemical energy storage. Ionics, 2023, 29(6), 2099-2113.

[9] Ma, CK., Chen, HL., Wang, C., Zhang, JF., Qi, H., Zhou, LM. Effects of Nano-Aluminum Nitride on the Performance of an Ultrahigh-Temperature Inorganic Phosphate Adhesive Cured at Room Temperature. Materials, 2017, 10(11).

[10] Wagh, A. Inorganic phosphate performance coatings. Abstracts of papers of the american chemical society, 2016, 251(71).

[11] Pourhashem, S., Saba, F., Duan, JZ., Rashidi, A., Guan, F., Nezhad, EG., Hou, BR. Polymer/Inorganic nanocomposite coatings with superior corrosion protection performance: A review. Journal of industrial and engineering chemistry, 2020, 88, 29-57.

[12] Xian, YB., Zhang, Y., Chen, L., Wu, YP., Zhou, HD., Chen, JM. Improvement on toughness and tribological properties for phosphate bonded MoS2 coatings by introduction of polytetrafluoroethylene. Journal of materials research, 2022, 37(15), 2446-2457.

[13] Ding, F., Chen, XH., Wei, DB., Tian, T., Zhang, PZ., Li, FK., Yang, K. Fatigue Behavior of 300 M Steel Coated with Water-Based Aluminum Phosphate Coating. Journal of materials engineering and performance, 2020, 29(10), 6661-6669.

[14] Wang, JT., Jiang, BC., Cao, JD. Corrosion Mechanism of Q235A under 3.5% NaCl Salt Spray. Materials transactions, 2020, 61(12), 2342-2347.

[15] Armstrong, G., Environmental and legislative impacts on anti-corrosion primers and paints: the use of anti-corrosive primers and coatings in aerospace applications. Transactions of the institute of metal finishing, 2022, 100(4), 178-180.

[16] Li, LC., Yin, Y., Wan, B., Luan, YG. Research on Flow Field Characteristics of an Artificial Seawater Spray Chambe. Journal of the chinese society of mechanical engineers, 2021, 42(1), 43-50.

[17] Zielecka, M., Zielecka, M., Zielecka, M., Zielecka, M. Flame Resistant Silicone-Containing Coating Materials. Coatings, 2020, 10(5), 479.

[18] Zielecka, M., Rabajczyk, A., Cyganczuk, K., Pastuszka, L., Jurecki, L. Silicone Resin-Based Intumescent Paints. Materials, 2020, 13(21), 4785.

[19] Mo, Yang In., Kang, Mijung., Lee, Sunmook., Kim, Hyun-A., Kim, Sangseok. Assessing the Reliability on Anti-Fouling and the Seawater-Erosion of Silicone-Based Anti-Fouling Coatings. Journal of Applied Reliability, 2020, 20(1), 63-71.

[20] Liu, YW., Wang, Z.,Liu, C.,Ma, JM. In depth analysis of corrosion mechanism of U-tube under conditions of differential aeration. Journal of electroanalytical, 2022, 906.

[21] Hageman, T., Andrade, C., Martínez-Pañeda, E. Corrosion rates under charge-conservation conditions. Electrochimica acta, 2023, 461, 142624.

[22] Guo,D., Li, M., Joseph, JM., Wren, JC. A New Method for Corrosion Current Measurement: the Dual-Electrochemical Cell (DEC). Journal of the electrochemical society, 2020, 111505.

[23] Ariyoshi, K., Siroma, Z., Mineshige, A., Takeno, M., Fukutsuka, T., Abe, T., Uchida, S. Electrochemical Impedance Spectroscopy Part1 Fundamentals. Electrochemistry, 2022, 90(10), 102007.

[24] Self, EC., Delnick, FM., Sacci, RL., Nanda, J. Assessing Nonlinear Polarization in Electrochemical Cells using AC Impedance Spectroscopy. Journal of the electrochemical society, 2024, 171(3), 030513.

[25] Varnosfaderani, MA., Strickland, D. A Comparison of Online Electrochemical Spectroscopy Impedance Estimation of Batteries. Ieee access, 2018, 6, 23668-23677.

[26] Dhillon, S., Kant, R. Theory for electrochemical impedance spectroscopy of heterogeneous electrode with distributed capacitance and charge transfer resistance. Journal of chemical sciences, 2017, 129(8), 1277-1292.

[27] Kuratani, K., Fukami, K., Tsuchiya, H., Usui, H., Chiku, M., Yamazaki, S. Electrochemical Polarization Part 1: Fundamentals and Corrosion. Electrochemistr, 2022, 90(20), 102003.

[28] Gómez, G., Argumosa, P., Correro, A., Maellas, J. Proposal of a New Technique to Obtain Some Fuel Cell Internal Parameters Using Polarization Curve Tests and EIS Results. Energies, 2021, 14, 21.

[29] Rybalka, KV., Beketaeva, LA., Davydov, AD. Estimation of corrosion current by the analysis of polarization curves: Electrochemical kinetics mode. Russian journal of electrochemistry, 2014, 50(2), 108-113.